Monitor for Detection and Analysis of Electrons and Ions in Geostationary Orbit Satellites

O. Anticura, J. Ascolani-Yael, G. Bagur, J. De Pellegrin, P.D. Fainstein, M. Famá[1], O. Grizzi
G. Lantschner, R. Mayer, D. Salazar-Alarcón, E.A. Sánchez, E. Sauro, A. Tartaglione.
Centro Atómico Bariloche - Comisión Nacional de Energía Atómica, Instituto Balseiro – Universidad Nacional de Cuyo, CONICET, Avda. Ezequiel Bustillo 9500, R8402AGP San Carlos de Bariloche, Río Negro, Argentina.
[1] AR-SAT, Avda. del Libertador 498 – P. 21 –C1001ABR Ciudad de Buenos Aires, Argentina.

We present a design for a monitor of space weather to be incorporated to an Argentinean geostationary orbit satellite. We show that within the budget of weight, energy consumption and telemetry imposed by the platform satellite it is possible to detect and analyze the energy of most of the electrons and ions responsible for the major satellite risks. A collection of measurements and estimates for the maximum and minimum expected fluxes is presented first. Due to the large span in these values we propose to implement a monitor with an array of three detector assemblies based on commercial surface barrier detectors (SBD).

Each detector has a specific combination of angular collimator, filter and type of SBDs. Calculations of slowing down and ranges of ions in solids as well as energy deposition in SBDs are used to choose an adequate combination of SBDs and shields for the selected energy thresholds. The set of detectors allows monitoring of the space weather in both the normal or low solar activity periods and also during the most intense periods known nowadays (1989). Finally, some remarks about the analog electronics and about the thermal behaviour of the detectors are provided.

Space Environment and design parameters of LEEP, PT and HEP detectors

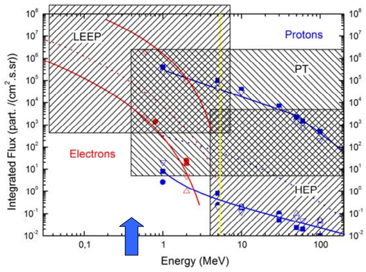

The maximum and minimum detector count rates (fixed by the time response of the analog electronic) define the spam of the integrated flux range

The angular aperture and the active surface area of the detector define the position of the integrated flux range

The entrance shield define the minimum energy of the detector

LOW ENERGY ELECTRON & PROTON DETECTOR (LEEP)
e^-: 0.03 < E < 1 MeV, H^+: 0.8 < E < 20 MeV. α: 2.8 < E < 75 MeV

Collection area (mm²)	Angular aperture (°)	SBD thickness (μm)	Al foil thickness (μm)	Nd magnets	Flux range (part / (cm².s.sr))
7	4	2000	10	no	$3x10^2$ to $2x10^8$

PARTICLE TELESCOPE DETECTOR (PT)
e^-: E > 5 MeV, H^+: E > 0.4 MeV, α: E > 1.4 MeV

Collection area (mm²)	Angular aperture (°)	SBD thickness (μm)	Al foil thickness (μm)	Nd magnets	Flux range (part / (cm².s.sr))
50	14	2000 500	4	yes	4 to $2x10^6$

HIGH ENERGY PROTON DETECTOR (HEP)
e^-: E > 4 MeV, H^+: E > 40 MeV. α: E > 150 MeV

Collection area (mm²)	Angular aperture (°)	SBD thickness (μm)	W foil thickness (μm)	Nd magnets	Flux range (part / (cm².s.sr))
300	120	500	1570	no	$1x10^{-2}$ to $5x10^3$

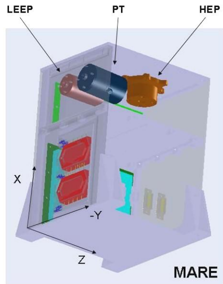

LEEP

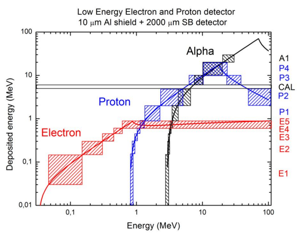

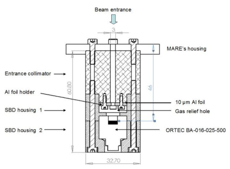

Bin	Electrons			Protons			Alfas		
	Incoming energy (MeV)	Minimum count rate (Counts/s)	Maximum count rate (Counts/s)	Incoming energy (MeV)	Minimum count rate (Counts/s)	Maximum count rate (Counts/s)	Incoming energy (MeV)	Minimum count rate (Counts/s)	Maximum count rate (Counts/s)
E1	0.03 < E < 0.15	1.20	120000	0.80 < E < 0.85	0.0011	75	2.8 < E < 3.0	0.000005	0.40
E2	0.15 < E < 0.30	0.01	1000	0.85 < E < 0.93			3.0 < E < 3.1		
E3	0.3 < E < 0.45	0.022	2200	0.93 < E < 1.02			3.1 < E < 3.17		
E4	0.45 < E <0.60	0.011	1100	1.02 < E < 1.13	0.0009	60	3.17 < E < 3.37	0.00001	0.80
E5	0.60 < E	0.0061	615	1.13 < E < 1.3			3.37 < E < 3.42		
P1				1.3 < E < 2.2			3.42 < E < 4.3		
P2				2.2 < E < 5 50 < E	0.0003 0.00001	20 1	4.3 < E < 6.4	0.000008	0.64
CAL							5.5 Am source 220		1.5 max
P3				6 < E < 10 24 < E <37	0.00022 0.00003	15 2	10 < E < 20	0.000004	0.32
P4				10 < E < 24	0.00015	10	10 < E < 20	0.000004	0.32
A1							20 < E < 30	----	0.05

PT

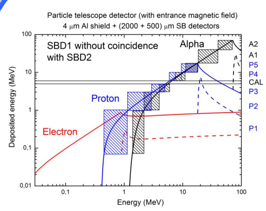

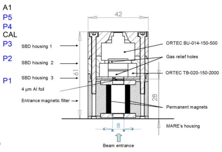

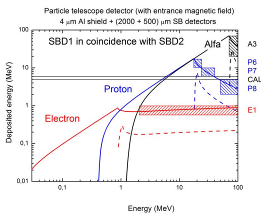

Bin	Electrons			Protons			Alfas		
	Incoming energy (MeV)	Minimum count rate (Counts/s)	Maximum count rate (Counts/s)	Incoming energy (MeV)	Minimum count rate (Counts/s)	Maximum count rate (Counts/s)	Incoming energy (MeV)	Minimum count rate (Counts/s)	Maximum count rate (Counts/s
E1	4 << E	0.0006	60						
P1				0.4 < E < 1.2	0.83	55000	1.4 < E < 2.2	0.0018	144
P2				1.2 < E < 3	0.06	4000	2.2 < E < 3	0.0014	112
P3				3 < E < 5	0.024	1600	3 < E < 6	0.0015	120
P4				6 < E < 10	0.02	1300	7.5 < E < 11	0.0005	40
P5				10 < E < 17	0.011	700	11 < E < 17	0.00025	20
P6				17 < E < 30	0.006	400			
P7				30 < E < 50	0.003	160			
P8				50 < E < 100	0.001	80			
CAL							5.5 Am source 220	9 max	9 max
A1							17 < E < 40	0.00009	7
A2							40 < E < 70	0.000009	0.7
A3							70 < E	0.000002	0.02

HEP

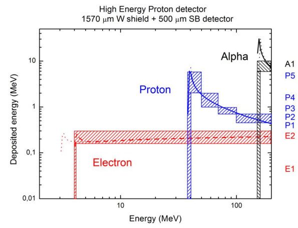

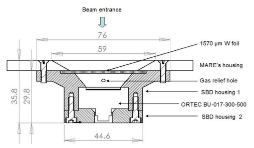

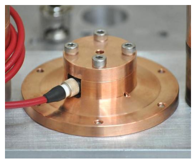

Bin	Electrons			Protons			Alfas		
	Incoming energy (MeV)	Minimum count rate (Counts/s)	Maximum count rate (Counts/s)	Incoming energy (MeV)	Minimum count rate (Counts/s)	Maximum count rate (Counts/s)	Incoming energy (MeV)	Minimum count rate (Counts/s)	Maximum count rate (Counts/s)
E1	4	0.15	15000 (integ. 3.8-4 MeV)	40	0.25	10400 (integ. 35/40 MeV)	150	0.000045	3.6
E2	4 < E	0.25	25000	40 400 < E	No data	No data	150		
P1				40 200 < E < 300	0.011	460	150		
P2				40 100 < E < 200	0.13	5250	150		
P3				40 70 < E < 100	0.19	7625	150		
P4				40 50 < E < 70	0.33	13240	150 500 < E	0.000004	0.32
P5				40 < E < 50	0.34	13800	150 250 < E < 500	0.000023	1.8
CAL							5.5 MeV ^{241}Am source 220	18 max	18 max
A1							150 < E < 220	0.00027	56

Evaluation of the analog detection proposals

Measurements of pile-up produced by the increasing count rate. This was evaluated with a random pulse generator and an alpha source for the two proposed analog detection chains (a) Without BLR (b) With BLR.

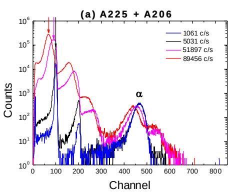

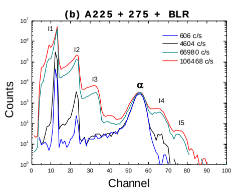

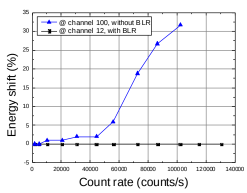

Percentage of energy shift vs particle counting rate for the two detection chains.

SBD thermal response

Simulation of the detector temperature variation along the orbital trajectory

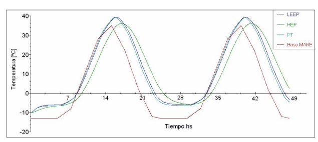

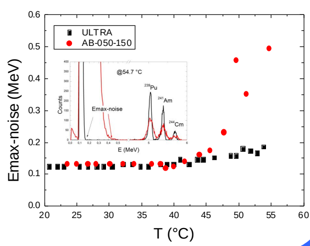

We acknowledge partial support from the SeCTyP-UNCuyo (06/C383), ARSAT S.A., MinCyT (PID 2008-00008 and PICT 903/07); mechanical and thermal design, and simulations from UID-GEMA-UNLa Plata; and technical assistance from INVAP S.E.